

Cramer-Rao Bounds for Target Position and Velocity Estimations for Widely Separated MIMO Radar

Yılmaz KALKAN

Department of Electronics and Communication Engineering, Süleyman Demirel University, Isparta, Turkey

yilmazkalkan@sdu.edu.tr

Abstract. *In this paper, we derive the Cramer-Rao Bounds (CRBs) for the 2-dimensional (2D) target localization and velocity estimations for widely separated Multiple-Input Multiple-Output (MIMO) radar. The transmitters emit signals with different frequencies and the receivers receive these signals with amplitude fluctuations and with Doppler shifts due to the target motion. The received signal model is constructed using the Swerling target fluctuations to take into account the undesired effects of target amplitude and phase fluctuations. Moreover, the time delays and the Doppler frequencies are included in the signal model to get a more realistic model. Then, the Cramer-Rao Bounds are derived for the proposed signal model for the target position and velocity estimations. Contrary to known models of CRBs, we derived the CRBs jointly and using the Swerling target fluctuations.*

Keywords

CRB, MIMO radar, target localization, velocity estimation, Swerling target fluctuations, Doppler frequency.

1. Introduction

Being able to place a lower bound on the variance of any unbiased estimator proves to be extremely useful in practice [1]. At worst, it provides a benchmark against which we can compare the performance of any unbiased estimator. Although many such variance bounds exist, the Cramer-Rao Bound (CRB) is by far the easiest to determine. Also, the theory allows us to determine if an estimator exists that attains the bound.

In general, the CRB derivations are nearly same for all applications. A received signal model is used for calculations, then Fisher Information Matrix (FIM) is calculated using the probability density functions (pdf) of the received signal with respect to the unknowns. The main difference is seen in the construction of the received signal model which depends on the application such as radar, sonar or wireless

sensor networks etc. Received signal includes information (time delay, Doppler shift, power etc.) about the unknown parameters (range, position, direction, velocity etc.) of target which are desired to be estimated. In [2] and [3], Time of Arrival (TOA) information is used to calculate the CRB for target range estimation in sensor networks. In [4], the CRB of localization accuracy for Received Signal Strength (RSS) is derived based on the Radio Frequency (RF) power measurements in WLAN environments. Similarly, CRB is derived for indoor range estimation using Doppler frequency in [5]. In [6], multistatic radar scenario and the bistatic CRBs are derived on the estimation accuracy of the target range and velocity. The CRB with uncertain observations (when the probability of detection is less than 1) is analyzed in [7] for target localization problem. The CRB for target's Doppler and power when detecting targets using space-based radar platform is investigated in [8] when a target's azimuth and elevation are both known.

The CRB derivations for MIMO radar is very limited in the literature. In [9], target localization methods for the MIMO radar are summarized, and the CRB is derived. In the same paper, the MIMO radar for widely separated case is investigated and the target localization is performed using only Time-of-Arrival (TOA) information. Similarly in [10], the CRB is derived when there is a phase error in coherent processing. In [11, 12], the CRBs are analyzed for MIMO radar with widely separated antennas individually. In [11], the CRB for target position estimation is derived using time delays but the Doppler frequency shift is not included in signal model. Similarly, the CRB is investigated for target velocity estimation using the Doppler frequency in [12]. The target velocity estimation with distributed MIMO radars in non-homogeneous environment is investigated in [13] and exact and asymptotic CRBs are calculated. In [14], the CRB including the antenna parameters is derived and then the effects of a four-element linear array are explored for target's direction estimation. In [15], the target localization is investigated and the CRB is derived for distributed MIMO radars by using dual frequency Continuous Wave (CW) radars. Moreover, in the same paper, the target amplitude fluctuations are assumed constant in the observation time.

In this paper, the received signals are constructed using the Swerling target fluctuations [16] to take into account the undesired effects of target amplitude and phase fluctuations for widely separated MIMO radar. Moreover, the time delays and the Doppler frequencies are included in the signal model to get a more realistic model. Then, the Cramer-Rao Bounds are derived for the proposed signal model for the target position and velocity estimations. Contrary to known models of CRBs, we derived the CRBs jointly and using the Swerling target fluctuations which are quite realistic models for received signals for MIMO radar.

The rest of the paper is organized as follows. In Section 2, the signal model is constructed. Section 3 includes the derivation of the CRBs for target position and velocity estimations. Simulation results are presented in Section 4 and conclusions are given in Section 5.

2. Signal Model

Let N_T transmitters arbitrarily located at $T_j = (x_{Tj}, y_{Tj})$ for $j = 1, 2, \dots, N_T$. The signals scattered by the target at (x, y) are collected by N_R receivers placed at arbitrary coordinates $R_i = (x_{Ri}, y_{Ri})$ for $i = 1, 2, \dots, N_R$. The set of transmitted waveforms in lowpass equivalent form is $\sqrt{E_e} s_k(t)$ for $k = 1, 2, \dots, N_T$ where $\int_0^T |s_k(t)|^2 dt = 1$ and $E_e = E/N_T$ is the normalized transmitted energy while E is the total transmitted energy, and T is the observation interval. N_T transmitters emit unmodulated, continuous wave (CW) tone signals in different frequencies which are f_1, f_2, \dots, f_{N_T} , and N_R receivers intercept these signals as attenuated and time delayed with Doppler-shifted frequencies due to the target motion. The received signal by the l^{th} receiver can be written as

$$r_l(t) = \sqrt{E_e} \sum_{k=1}^{N_T} A_{lk}(t) s_k(t - \tau_{lk}) \exp(-j2\pi(f_k + f_{d_{lk}})(t - \tau_{lk})) + w_l(t) \quad (1)$$

where f_k is the carrier frequency of the k^{th} transmitter, $f_{d_{lk}}$ and τ_{lk} are the Doppler frequency and time delay from the k^{th} transmitter to the target and from the target to the l^{th} receiver respectively. $A_{lk}(t)$ is the complex target fluctuations which is modeled using the Swerling target fluctuations and $w_l(t)$ is the spatially and temporarily White, circularly symmetric, zero mean Gaussian noise with autocorrelation function $\sigma_w^2 \delta(\tau)$.

3. Cramer-Rao Bound

The CRB provides a lower bound for the mean square error (MSE) of any unbiased estimator for unknown parameters. Given a vector parameter θ , its unbiased estimate $\hat{\theta}$ satisfies the following inequality [1]

$$E_{\theta} \left\{ (\hat{\theta}_i - \theta_i)(\hat{\theta}_i - \theta_i)^T \right\} \geq [J^{-1}(\theta)]_{i,i} \quad (2)$$

where $J(\theta)$ is the Fisher Information matrix (FIM) given as

$$J(\theta) = E_{\theta} \left\{ \frac{d}{d\theta} \log p(\mathbf{r}|\theta) \left(\frac{d}{d\theta} \log p(\mathbf{r}|\theta) \right)^T \right\} \quad (3)$$

where $p(\mathbf{r}|\theta)$ is the joint probability density function of \mathbf{r} given θ . The vector of unknowns is defined as $\theta \triangleq [x, y, V_x, V_y]^T$ for the target localization problem in two dimensional space. After the FIM is calculated, the CRB matrix can be found as

$$\mathbf{C}_{CRB} = [\mathbf{J}^{-1}(\theta)]. \quad (4)$$

The bounds for the unknown parameters (x, y, V_x, V_y) are on the main diagonal of this matrix as

$$C_{CRB_x} = \mathbf{C}_{CRB}(1, 1), \quad (5)$$

$$C_{CRB_y} = \mathbf{C}_{CRB}(2, 2), \quad (6)$$

$$C_{CRB_{V_x}} = \mathbf{C}_{CRB}(3, 3), \quad (7)$$

$$C_{CRB_{V_y}} = \mathbf{C}_{CRB}(4, 4), \quad (8)$$

and the target position and velocity estimation bounds can be calculated as

$$CRB_{loc} = \sqrt{C_{CRB_x}^2 + C_{CRB_y}^2}, \quad (9)$$

$$CRB_{vel} = \sqrt{C_{CRB_{V_x}}^2 + C_{CRB_{V_y}}^2}. \quad (10)$$

3.1 Calculation of Fisher Information Matrix

In the case of Gaussian observations, the CRB can be derived as shown in [1]. In the baseband and after sampling with period of T_s , the received narrowband signal at the l^{th} receiver can be written as

$$r_l[n] = s_l[n, \theta] + w_l[n]; \quad n = 1, 2, \dots, N \quad (11)$$

where

$$s_l[n, \theta] = \sqrt{E_e} \sum_{k=1}^{N_T} A_{lk}[n] s_k[n] \exp\left(-j2\pi f_{d_{lk}} T_s \left(n - \frac{\tau_{lk}}{T_s}\right)\right) \quad (12)$$

and

$$\mathbf{r}_l = [r_l[1], r_l[2], \dots, r_l[N]]; \quad l = 1, 2, \dots, N_R, \quad (13)$$

$$\mathbf{s}_l(\theta) = [s_l[1, \theta], \dots, s_l[N, \theta]]; \quad l = 1, 2, \dots, N_R. \quad (14)$$

The exact received signal is the combination of all received signals as follows

$$\mathbf{r} = [\mathbf{r}_1, \mathbf{r}_2, \dots, \mathbf{r}_{N_R}]^T \quad (15)$$

and similarly

$$\mathbf{s}(\boldsymbol{\theta}) = [\mathbf{s}_1(\boldsymbol{\theta}), \mathbf{s}_2(\boldsymbol{\theta}), \dots, \mathbf{s}_{N_R}(\boldsymbol{\theta})]^T. \quad (16)$$

Hence, $p(\mathbf{r}|\boldsymbol{\theta}) \sim N(\boldsymbol{\mu}(\boldsymbol{\theta}), \boldsymbol{\sigma}^2)$ where $\boldsymbol{\theta} = [x, y, V_x, V_y]^T$ and $\mathbf{C}(\boldsymbol{\theta}) = \boldsymbol{\sigma}^2 \mathbf{I}_{N_R \times N_R}$. The elements of FIM can be written as

$$[J(\boldsymbol{\theta})]_{ij} = \frac{2}{\boldsymbol{\sigma}^2} \text{Re} \left\{ E \left[\left[\frac{d\mathbf{s}(\boldsymbol{\theta})}{d\theta_i} \right]^H \left[\frac{d\mathbf{s}(\boldsymbol{\theta})}{d\theta_j} \right] \right] \right\} \quad (17)$$

where $(\theta_i, \theta_j) \in (x, y, V_x, V_y)$, $E[\cdot]$ shows the expected value operation and

$$\frac{d\mathbf{s}(\boldsymbol{\theta})}{d\boldsymbol{\theta}} = \begin{bmatrix} \frac{ds_1(\boldsymbol{\theta})}{dx} & \frac{ds_1(\boldsymbol{\theta})}{dy} & \frac{ds_1(\boldsymbol{\theta})}{dV_x} & \frac{ds_1(\boldsymbol{\theta})}{dV_y} \\ \frac{ds_2(\boldsymbol{\theta})}{dx} & \frac{ds_2(\boldsymbol{\theta})}{dy} & \frac{ds_2(\boldsymbol{\theta})}{dV_x} & \frac{ds_2(\boldsymbol{\theta})}{dV_y} \\ \dots & \dots & \dots & \dots \\ \frac{ds_{N_R}(\boldsymbol{\theta})}{dx} & \frac{ds_{N_R}(\boldsymbol{\theta})}{dy} & \frac{ds_{N_R}(\boldsymbol{\theta})}{dV_x} & \frac{ds_{N_R}(\boldsymbol{\theta})}{dV_y} \end{bmatrix}.$$

These derivatives can be calculated as

$$\frac{ds_l[n, \boldsymbol{\theta}]}{d\theta_i} = -j2\pi T_s s_l[n, \boldsymbol{\theta}] \left(\frac{d\alpha_{l,k}}{d\theta_i} \right) \quad (18)$$

where $\alpha_{l,k} = f_{d_{lk}}(n - \frac{\tau_{lk}}{T_s})$ and

$$f_{d_{lk}} = \frac{f_k}{C} \left(\frac{(x - x_{T_k})V_x + (y - y_{T_k})V_y}{\sqrt{(x - x_{T_k})^2 + (y - y_{T_k})^2}} \right) + \frac{f_k}{C} \left(\frac{(x - x_{R_l})V_x + (y - y_{R_l})V_y}{\sqrt{(x - x_{R_l})^2 + (y - y_{R_l})^2}} \right), \quad (19)$$

$$\tau_{lk} = \frac{\sqrt{(x - x_{T_k})^2 + (y - y_{T_k})^2}}{C} + \frac{\sqrt{(x - x_{R_l})^2 + (y - y_{R_l})^2}}{C} \quad (20)$$

where C is the speed of light. The required derivatives can be calculated as

$$\frac{d\alpha_{l,k}}{dx} = \left(n - \frac{\tau_{lk}}{T_s} \right) \frac{df_{d_{lk}}}{dx} - \frac{f_{d_{lk}}}{T_s} \frac{d\tau_{l,k}}{dx}, \quad (21)$$

$$\frac{d\alpha_{l,k}}{dy} = \left(n - \frac{\tau_{lk}}{T_s} \right) \frac{df_{d_{lk}}}{dy} - \frac{f_{d_{lk}}}{T_s} \frac{d\tau_{l,k}}{dy}, \quad (22)$$

$$\frac{d\alpha_{l,k}}{dV_x} = \left(n - \frac{\tau_{lk}}{T_s} \right) \frac{df_{d_{lk}}}{dV_x}, \quad (23)$$

$$\frac{d\alpha_{l,k}}{dV_y} = \left(n - \frac{\tau_{lk}}{T_s} \right) \frac{df_{d_{lk}}}{dV_y}. \quad (24)$$

By using these equations, the elements of the FIM can be calculated by rewriting (17) as

$$[J(\boldsymbol{\theta})]_{ij} = \frac{2}{\boldsymbol{\sigma}^2} \text{Re} \{ E \{ \Psi \} \} \quad (25)$$

where

$$\begin{aligned} \Psi &= \left[\frac{d\mathbf{s}(\boldsymbol{\theta})}{d\theta_i} \right]^H \left[\frac{d\mathbf{s}(\boldsymbol{\theta})}{d\theta_j} \right] \\ &= \sum_{l=1}^{N_R} \sum_{n=1}^N \left[\frac{ds_l[n, \boldsymbol{\theta}]}{d\theta_i} \right]^H \left[\frac{ds_l[n, \boldsymbol{\theta}]}{d\theta_j} \right] \end{aligned} \quad (26)$$

and

$$\begin{aligned} \Psi &= 4E_e(\pi T_s)^2 \sum_{l=1}^{N_R} \sum_{n=1}^N \sum_{k=1}^{N_T} \sum_{m=1}^{N_T} A_{lk}^*[n] A_{lm}[n] s_k^*[n] s_m[n] \\ &\times \exp(j2\pi T_s(\alpha_{l,m} - \alpha_{l,k})) \left(\frac{d\alpha_{l,k}}{d\theta_i} \right) \left(\frac{d\alpha_{l,m}}{d\theta_j} \right). \end{aligned} \quad (27)$$

From the equations above, it can be written as

$$\begin{aligned} E \{ \Psi \} &= 4E_e(\pi T_s)^2 \sum_{l=1}^{N_R} \sum_{n=1}^N \sum_{k=1}^{N_T} \sum_{m=1}^{N_T} \mu_{k,m}[n] s_k^*[n] s_m[n] \\ &\times \exp(j2\pi T_s(\alpha_{l,m} - \alpha_{l,k})) \left(\frac{d\alpha_{l,k}}{d\theta_i} \right) \left(\frac{d\alpha_{l,m}}{d\theta_j} \right) \end{aligned} \quad (28)$$

where

$$\mu_{k,m}[n] = E \{ A_{lk}^*[n] A_{lm}[n] \} \quad (29)$$

and

$$\mu_{k,m}[n] = \begin{cases} R_A(0); & k = m, \\ E \{ A_{lk}^*[n] \} E \{ A_{lm}[n] \} = 1; & k \neq m \end{cases} \quad (30)$$

where $R_A(0) = E \{ |A_{lk}[n]|^2 \}$ denotes the average power in the process $A_{lk}[n]$. It can be written that

$$\begin{aligned} E \{ \Psi \} &= 4E_e(\pi T_s)^2 R_A(0) \sum_{l=1}^{N_R} \sum_{n=1}^N \sum_{k=1}^{N_T} |s_k[n]|^2 \left(\frac{d\alpha_{l,k}}{d\theta_i} \right) \left(\frac{d\alpha_{l,k}}{d\theta_j} \right) \\ &+ 4E_e(\pi T_s)^2 \sum_{l=1}^{N_R} \sum_{n=1}^N \sum_{k=1}^{N_T} \sum_{\substack{m=1 \\ m \neq k}}^{N_T} s_k^*[n] s_m[n] \\ &\times \exp(j2\pi T_s(\alpha_{l,m} - \alpha_{l,k})) \left(\frac{d\alpha_{l,k}}{d\theta_i} \right) \left(\frac{d\alpha_{l,m}}{d\theta_j} \right) \end{aligned} \quad (31)$$

and finally, the elements of the FIM can be obtained as

$$J_{ij} = \frac{8E_e(\pi T_s)^2}{\boldsymbol{\sigma}_n^2} R_A(0) \sum_{l=1}^{N_R} \sum_{k=1}^{N_T} \sum_{n=1}^N \left(\frac{d\alpha_{l,k}}{d\theta_i} \right) \left(\frac{d\alpha_{l,k}}{d\theta_j} \right). \quad (32)$$

4. Simulations

The Cramer Rao Bounds for the target localization and the target velocity estimation depend on the geometry of the system. The system geometry includes the positions and the numbers of the targets, transmitters and receivers. Hence, the system geometry should be defined in order to evaluate the target localization performance. In Fig. 1, the simulation geometry used for the CRB simulations can be seen.

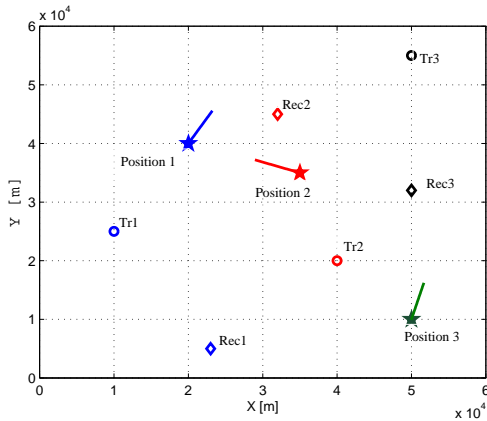


Fig. 1. System geometry used for the CRB simulations.

In this simulation geometry, target is assumed at three different positions and directions with $V = 800$ kmph velocity. For 2×2 MIMO radar Tr1, Tr2, Rec1 and Rec2 are used as transmitter and receiver pairs. For 2×3 MIMO radar, Rec3 is added, and for 3×3 MIMO radar, Tr3 is added to the geometry. The used transmitter frequencies are, 10, 10.3 and 10.5 GHz for Tr_1, Tr_2 and Tr_3 respectively. The observation time is chosen as $T = 1, 10, 100$ msec and time delays (τ_{lk}) and the Doppler frequencies (f_{dlk}) are assumed as totally known.

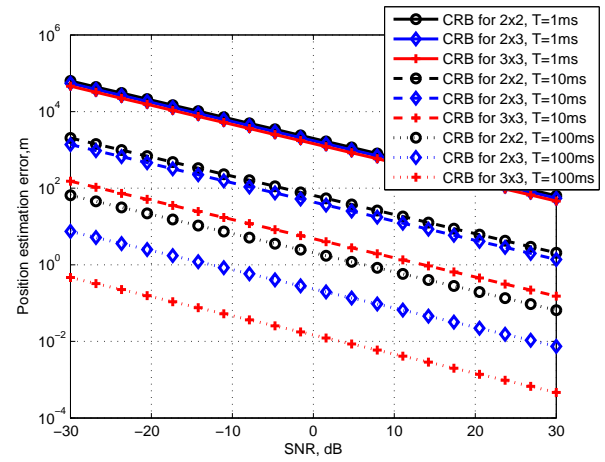
The maximum velocity of the target is chosen as $V_{max} = 900$ kmph = 250 m/sec and the maximum carrier frequency is chosen as 10.5 GHz. For these settings, the maximum Doppler frequency can be calculated as

$$f_{dmax} = 2 \frac{V_{max}}{C} f_{max} = 17.5 \text{ kHz.} \quad (33)$$

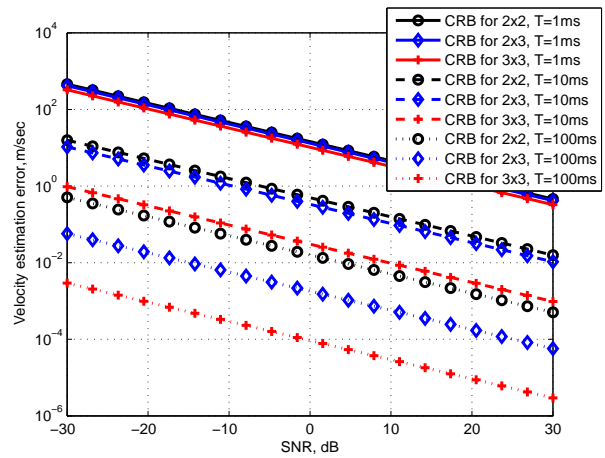
Hence, the sampling frequency is used as $f_s = 35$ kHz which is the Nyquist sampling frequency. For all three cases, including Swerling 2, Swerling 4 and no fluctuation cases, $R_A(0) = 1$. It turns out that, the CRBs are the same, because the CRB depends only on the value of $R_A(0)$.

In Figs. 2 and 3, the CRBs for different observation times can be seen for different target positions. As expected, when the observation time increases, the bound decreases because the extra information increases the estimation performance. Similarly, bounds decrease when the number of transmit and/or receive sites increases. On the other hand, these figures show that the CRB depends not only on the positions of the transmitters and receivers but also on the parameters of the target such as position, velocity and direction.

In Figs. 4, and 5, the CRBs can be seen for targets at position2 and position3 with different directions. Targets are assumed at position2 and position3 with $V = 800$ kmph and the direction of the target is scanned from 0 to 2π . For these simulations, the observation time and the SNR are chosen as 10 ms and 0 dB respectively. As seen from these figures, direction of the target effects CRB especially for 2×2 MIMO radar case. When the number of transmitters and/or receivers increase, the effect of target's parameters on CRBs decrease. It is an expected result because the position, velocity and the direction of the target directly effect the produced Doppler frequency and hence the target localization performance. When the system includes 2 transmitters and 2 receivers, only 4 Doppler frequencies are obtained and the effect of each of them is large. On the other hand, when the system includes 3 transmitters and 3 receivers, 9 Doppler frequencies are obtained and the effect of each of them decreases and bounds close to the constant. As a result, the number of radar units should be increased to achieve better localization performance.

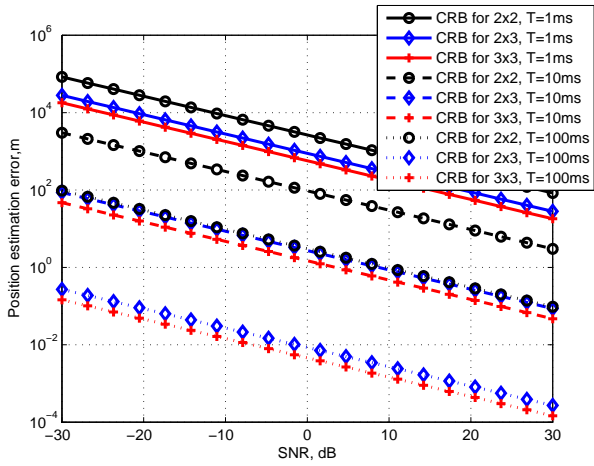


(a) CRB for position.

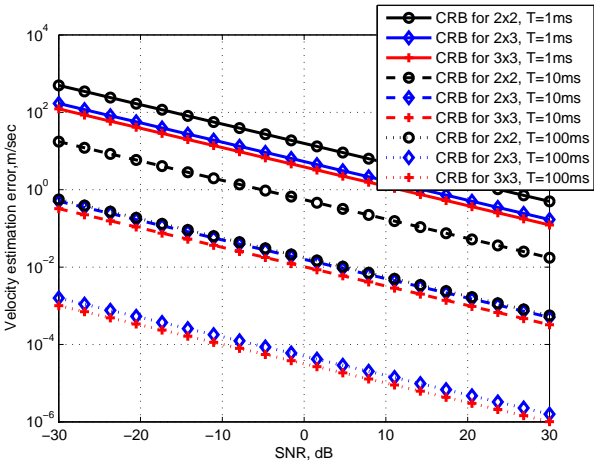


(b) CRB for velocity.

Fig. 2. CRBs for target position and velocity estimation when target is at position1.

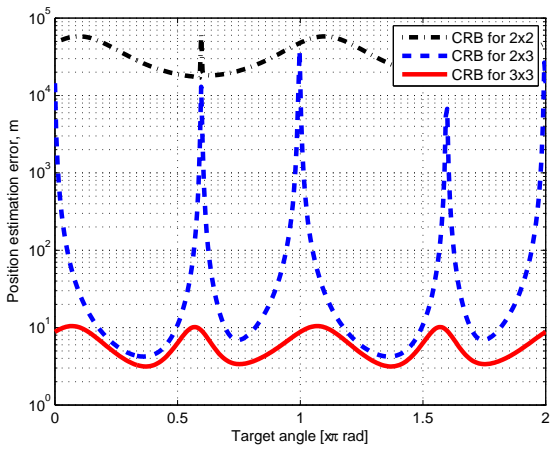


(a) CRB for position.

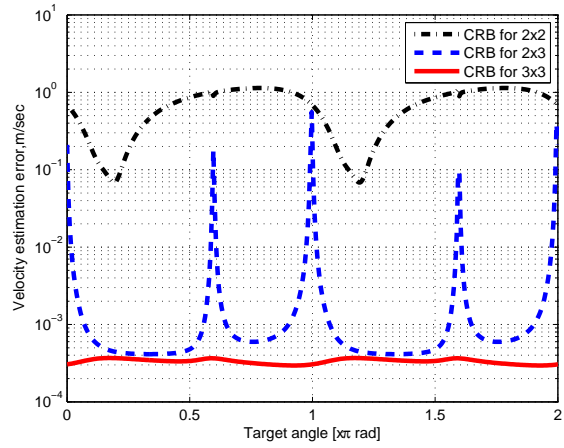


(b) CRB for velocity.

Fig. 3. CRBs for target position and velocity estimation when target is at position2.

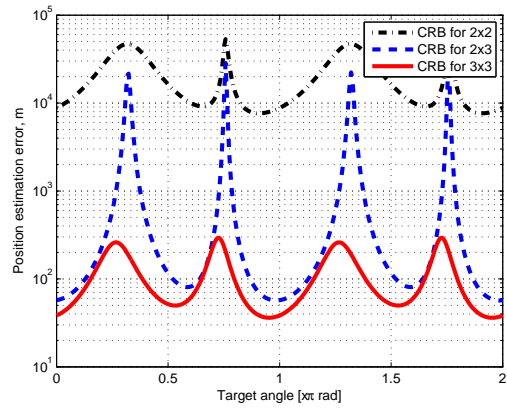


(a) CRB for position.

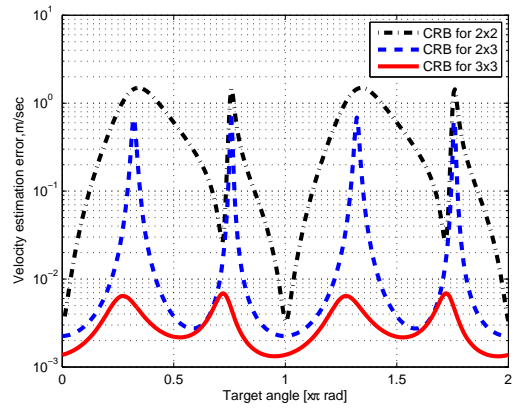


(b) CRB for velocity.

Fig. 4. CRBs for target position and velocity estimation when target is at position2, $T = 10$ ms, $SNR = 0$ dB, and direction is changed from 0 to 2π .



(a) CRB for position.



(b) CRB for velocity.

Fig. 5. CRBs for target position and velocity estimation when target at position3, $T = 10$ ms, $SNR = 0$ dB, and direction is changed from 0 to 2π .

5. Conclusion

In this paper, the Cramer-Rao Bounds for widely separated MIMO radar for the target position and velocity estimations are derived jointly. The theoretical results have been supported with simulation results. The Swerling target amplitude fluctuations and the Doppler frequencies are included in the received signal model in order to obtain a realistic radar signal model. The obtained results are simulated using 2×2 , 2×3 and 3×3 MIMO radar configurations and different target positions. As expected, increasing the number of transmitters and/or receivers decreases the bound. Similarly, large observation time gives lower bounds. On the other hand, the computational complexity increases as dealing with the longer data stream. Hence, the observation time should be chosen properly. Very long observation time gives better result but computational load shouldn't be forgotten. If the observation time is chosen very small, then one period of the baseband signal couldn't be covered and the correct position of the target can not be estimated. Finally, it is shown that, Cramer-Rao Bounds for target position and velocity estimations depend on the system geometry (radar locations) and the position and the direction of the target. It is advisable, in the system design phase, in order to find optimal positioning of transmitters and receivers, which should give as low CRB as possible.

References

- [1] KAY, S. M. *Fundamentals of Statistical Signal Processing: Estimation Theory, Vol. 1*. Upper Saddle River (NJ, USA): Prentice Hall, 1993.
- [2] JIA, T., BUEHRER, R. M. A new Cramer-Rao lower bound for TOA-based localization. In *Military Communications Conference MILCOM 2008*. San Diego (CA, USA), 2008, p. 1 - 5.
- [3] KAUNE, R., HORST, J., KOCH, W. Accuracy analysis for TDOA localization in sensor networks. In *14th International Conference on Information Fusion, FUSION 2011*. Chicago (IL, USA), 2011, p. 1 - 8.
- [4] STELLA, M., RUSSO, M., BEGUSIC, D. RF localization in indoor environment. *Radioengineering*, 2012, vol. 21, no. 2, p. 557 - 567.
- [5] SETLUR, P., AMIN, M., AHMAD, F. Dual-frequency Doppler radars for indoor range estimation: Cramer-Rao bound analysis. *IET Signal Processing*, 2010, vol. 4, p. 256 - 271.
- [6] GRECO, M. S., STINCO, P., GINI, F., FARINA, A. Cramer-Rao bounds and selection of bistatic channels for multistatic radar systems. *IEEE Transactions on Aerospace and Electronic Systems*, 2011, vol. 47, no. 4, p. 2934 - 2948.
- [7] ANASTASIO, V., COLONE, F., DI LALLO, A., FARINA, A., GUMIERO, F., LOMBARDO, P. Optimization of multistatic passive radar geometry based on CRLB with uncertain observations. In *European Radar Conference EURAD 2010*. Paris (France), 2010, p. 340 - 343.
- [8] PILLAI, U. S., LI, K. Y., HIMED, B. Cramer-Rao bounds for target parameters in space-based radar applications. *IEEE Transactions on Aerospace and Electronic Systems*, 2008, vol. 44, no. 4, p. 1356 - 1370.
- [9] GODRICH, H., HAIMOVICH, A. M., BLUM, R. S. Target localization techniques and tools for multiple-input multiple-output radar. *IET Radar, Sonar & Navigation*, 2007, vol. 3, no. 4, p. 314 - 327.
- [10] HE, Q., BLUM, R. S. Cramer-Rao bound for MIMO radar target localization with phase errors. *IEEE Signal Processing Letters*, 2010, vol. 17, no. 1, p. 83 - 86.
- [11] GODRICH, H., HAIMOVICH, A. M., BLUM, R. S. Cramer Rao bound on target localization estimation in MIMO radar systems. In *42nd Annual Conference on Information Sciences and Systems, CISS 2008*. Princeton (NJ, USA), 2008, p. 134 - 139.
- [12] HE, Q., BLUM, R. S., GODRICH, H., HAIMOVICH, A. M. Cramer-Rao bound for target velocity estimation in MIMO radar with widely separated antennas. In *42nd Annual Conference on Information Sciences and Systems, CISS 2008*. Princeton (NJ, USA), 2008, p. 123 - 127.
- [13] WANG, P., LI, H., HIMED, B. Target velocity estimation and CRB with distributed MIMO radar in non-homogeneous AR-modeled disturbances. In *13th International Radar Symposium, IRS 2012*. Warsaw (Poland), 2012, p. 109 - 112.
- [14] XUAN, H. W., KISHK, A. A., GLISSON, A. W. Antennad'z's effects on a MIMO radar for angle estimation: A Cramer-Rao lower bound analysis. In *IEEE Antennas and Propagation Society International Symposium, AP-S 2008*. San Diego (CA, USA), 2008, p. 1 - 4.
- [15] JIN, M., LIAO, G., LI, J. Target localization for distributed multiple-input multiple-output radar and its performance analysis. *IET Radar, Sonar & Navigation*, 2010, vol. 5, p. 83 - 91.
- [16] RICHARDS, M. A. *Fundamentals of radar signal processing*. New York (USA): McGraw-Hill, 2005.

About Authors...

Yılmaz KALKAN was born in İzmir, Turkey in 1979. He received his B.S. degree in Electronics and Telecommunications Engineering from Kocaeli University, Kocaeli, Turkey and Ph.D. degree in Electrical Engineering from the Department of Electrical and Electronics Engineering, Middle East Technical University (METU), Ankara, Turkey in 2002 and 2012 respectively. Currently, he is a research assistant at the Electronics and Telecommunications Engineering Department, Süleyman Demirel University, Isparta, Turkey. His academic research interests include MIMO radar, radar signal processing, target tracking, statistical signal processing, and detection and estimation theory.